

# High-fidelity copying of large-area astronomical plates: principles and some practical results

M. P. van Haarlem,<sup>1</sup> R. S. Le Poole,<sup>1</sup> P. Katgert<sup>1</sup> and S. Tritton<sup>2</sup>

<sup>1</sup>Leiden Observatory, PO Box 9513, 2300 RA Leiden, The Netherlands

<sup>2</sup>UK Schmidt Telescope Unit, Royal Observatory, Blackford Hill, Edinburgh EH9 3HJ

Accepted 1991 October 15. Received 1991 October 11; in original form 1991 June 26

## SUMMARY

We report here on an investigation into the achieved fidelity of copies of a large Schmidt telescope plate. Atlas quality copies both on glass and film and the original are compared. Two glass copies made through different intermediate positives are used to look at the fidelity of the separate positives. We confirm the general belief that glass copies are capable of impeccable photogrammetric quality. However, film copies are shown to achieve essentially the same astrometric fidelity. The general feeling that for photometric applications film copies should be equivalent to glass ones is not confirmed. We find that glass copies are generally better in densitometry.

## 1 INTRODUCTION

With a new large-scale photographic survey presently underway, most astronomical institutes will have to decide shortly about the acquisition of copies of this new survey, as well as about the choice between glass and film copies. In this context, it is useful to have some quantitative information about the fidelity of copies in general and, more specifically, about the relative performance of glass and film copies.

We have made a study of the photometric and astrometric fidelity of several copies of a survey-quality IIIa-J plate made with the UK Schmidt Telescope at Siding Spring. As the copies were products of the standard copying procedures in use at the European Southern Observatory and in the UK Schmidt Telescope Unit, our comparison between an original and its copies should be relevant for the question of the respective merits of glass and film copies, even though our results pertain only to a single plate and its copies, and may therefore be illustrative rather than typical.

Since we could use an original glass negative, and several copy negatives some of which were made through a single intermediate positive, but others through a different intermediate positive, we have information about all stages of the copying process. For the photometric comparisons, we used quantities derived from large sets of individual photographic densities measured in elementary  $(10 \mu\text{m})^2$  pixels, which fully sample the point-spread function of the emulsion. By combining the values of many (order 1000) pixels one can suppress the noise in the individual pixels and relax the tolerances on the exact coincidence of pixels, so that we can reliably detect small differences between the photometric

properties of the original and its copies on scales down to a fraction of a millimetre. For the astrometric comparison we have used the averages of the position differences in areas of  $1 \text{ cm}^2$ , allowing us to detect small differences in the positional systems on the original and copies.

We have used the Leiden Observatory automatic plate-scanning machine Astroscan, which has very high photometric and positional accuracy and stability, as we demonstrate from repeated, fully independent measurements.

This paper is organized as follows. First, a discussion is given of the information content of a plate, and of the optimum way in which this should be copied, so as to yield an 'ideal copy'. Then we discuss the Astroscan hardware and software as it is relevant for an appreciation of our results. Finally, we describe the results of our study of photometric and astrometric fidelity of glass and film copies.

## 2 PLATE COPYING: WHAT MUST BE COPIED AND HOW?

For a copy of a scientific plate to be a 'high fidelity' copy of the original it is required that the full quantitative information is copied without significant degradation. This requirement makes it clear that an optimal copy does not necessarily look like the original from which it is copied. What is required, is that there exist calibratable transformations which allow one to reconstruct the original, both in photometry and in position, from the copy. The original should be recoverable from the copy without a significant enhancement of the noise and without unknown 'distortions', or equiva-

lently: the copying process should copy the noise of the original with a S/N ratio that is rather larger than unity and not 'add' unknown local deviations from the global transformations.

### 2.1 Information content of a photographic plate

A photographic record consists of grains of deposited silver which make up the image. The shot-noise in the silver deposit is the source of the noise in the photographic record. Microdensitometry is to a high degree of approximation the accurate measure of the spatial distribution of the surface density of these grains of silver. This is the explanation for the well-known property of photographic records to have a signal-to-noise ratio which increases proportionally with the square root of the area considered. At the same time it also explains the less well-known fact that this relation must break down beyond some scale.

Consider for instance a IIIa-J emulsion: the maximum S/N ratio for  $1000 \mu\text{m}^2$  is about 50. The area<sup>1/2</sup> law implies a S/N ratio of 1500 per  $\text{mm}^2$  (equivalent to almost 8 mag fainter than the sky for pixels of  $1 \text{ arcmin}^2$ ) on regular Schmidt plates or in principle a detectable variation of less than  $10^{-5}$  in the sky background on the scale of square degrees. Obviously, this level of uniformity of plate properties is not achievable in processing or even manufacture of the materials.

Some measurements of what *can* be achieved can be found in Latham (1978) and Millikan (1978). The implication is that from some spatial scale onward the variations in the properties of the developed image dominate the noise characteristics of the photographic record. Obviously, this applies not only to an original but to a copy as well, thereby restricting the inferences that can be made about an original from its copy.

The above discussion was given in terms of photometry, or rather, densitometry. It can easily be translated in terms of positional information. Consider again a Schmidt plate of IIIa-J type. A stellar image with characteristic dimensions of about  $30 \mu\text{m}$  (i.e. of area  $1000 \mu\text{m}^2$ ) provides a positional record with a quality of about  $1 \mu\text{m}$  (note the agreement with the S/N ratio achievable in densitometry). A plate can (and sometimes does) contain about 50 such objects per  $\text{mm}^2$  before confusion becomes the dominant source of problems. This means that if the quality of the mean of many objects would continue to be proportional to  $N^{1/2}$  for areas as large as significant fractions of a full plate, one should be able to measure mean positional differences for large sets of stars degrees apart (say 10 cm) to  $10^{-3} \mu\text{m}$  on scales of  $10^5 \mu\text{m}$ , or to a level of  $10^{-8}$ . Obviously, it is again unthinkable that this information quality can be extracted from photographic plates. With a thermal expansion coefficient of, e.g.,  $10^{-5} \text{ }^\circ\text{C}^{-1}$  this would require temperature management of the plate, both at exposure and during measurement, to millidegrees.

Other, more fundamental causes for the breakdown of the  $N^{1/2}$  relation are the thickness ( $\sim 25 \mu\text{m}$ ) of the emulsions commonly used (note that astronomical images are usually recorded only at the surface of the emulsion), and the flexure of the plate between exposure and read-out. With good care in the processing and careful management and description of physical plate distortions one may hope to keep these effects below a few tenths of a  $\mu\text{m}$ . It should be clear that flexure-

induced geometric distortions can very easily appear at a level of several  $\mu\text{m}$ , in particular in plate copying.

### 2.2 The 'ideal' plate copy

In producing a high-fidelity copy of an original photographic plate, one must of course try to ensure that the information content, as described above, can be fully extracted from the copy. This does not necessarily imply that the copy should look like the original as much as possible. Rather, one requires that there exist calibratable transformations (valid for the entire plate) which allow one to extract from the copy the same information that one can extract from the original.

A plate that was uniformly exposed may show non-uniformities on 'large scales' that are mainly due to effects in the processing. In *surface photometry* (the measurement of small  $\delta D$ ) the quality of a copy is determined by the degree to which  $\delta D$  in the copy carries the information of  $\delta D$  in the original. The variations in the background density of a copy are the result of two effects. First the variations in the original are copied with a 'gain' of  $\gamma_{\text{copy}}$ , the product of the  $\gamma$ 's at sky level of the intermediate positive and of the copy negative. Secondly the processed copy materials have intrinsic deviations from uniformity. The magnitude of these is only slightly dependent on the  $\gamma$  of the copy materials, and mainly depends on the care taken during the processing. Therefore, the degree to which variations in the background density of a copy reflect those in the original can be optimized by choosing materials with a high  $\gamma$  at the density of this background, both for the intermediate positive and for the copy negative.

In *object photometry* of small objects (stars and all but the nearer galaxies) the photometric information, which is equivalent to the ratio between the derivative of a photometric parameter ( $P$ ) with respect to magnitude ( $m$ ) and the noise in the photometric parameter, should be copied properly and without significant loss. This means that copying should not contribute noticeably to the noise in the photometric parameter and that  $dP/dm$  should be maximized.

As a result, it will be clear that the possible destructive influence in copying due to processing can be best suppressed by using a high  $\gamma$  in the copy at  $D_{\text{sky}}$  in the original, and especially in the intermediate positive. Clearly, such a high  $\gamma$  can and need only be maintained over a limited range in density and  $\gamma$  must inevitably decrease towards higher densities (or lower ones for the positive). The fact that copies made according to this prescription will not look very much like the original should now be appreciated as not very relevant, at least for microdensitometric evaluations.

Positional fidelity of copying is most likely limited by flexure introduced when original and copy are put in contact for exposure. Great care should therefore be taken to ensure that in contact printing the two plates are put into contact as stress-free as possible before evacuation is applied to improve, fix and maintain the contact.

## 3 THE ASTROSCAN AND ITS ON-LINE SOFTWARE

The Leiden Observatory automatic plate measuring machine (Astroscan) is a high-precision, multi-element microdensitometer capable of accurately digitizing photographic emulsions. The data can be pre-processed on-line, so that one

does not output the densities in all elementary ( $10\ \mu\text{m}$ )<sup>2</sup> pixels, but instead only derived quantities for background and detected objects. In this section we shall describe both the Astroscan hardware and its on-line software as far as is relevant for an understanding of the results of our comparisons.

### 3.1 The Astroscan hardware

The transmission of the photographic plate, which is illuminated by a current-stabilized Tungsten-halide lamp, is measured by a 128-element Reticon photodiode array. After correction for individual diode darkcurrents, gains and non-linearities, the transmissions are immediately converted to photographic densities using a look-up table. At the position of the emulsion the separation of the centres of adjacent diodes is  $10\ \mu\text{m}$ . The instrumental profile results in an effective area of each diode of about  $13^2\ \mu\text{m}^2$ . Thus the read-outs of neighbouring pixels are somewhat correlated.

The diode array is aligned along the  $x$ -axis of the table which supports the plate holder and the photographic plate. The design of the table is based on a David Mann monocomparator. Using two perpendicular screws driven by stepper motors the table can be moved in both directions. Each step of these stepper motors corresponds to a  $5\text{-}\mu\text{m}$  shift of the table with respect to the image of the array on the plate. The step size between measured pixels is always  $10\ \mu\text{m}$ . Optional binning to pixels with size equal to any integer multiple of  $10\ \mu\text{m}$  can be performed immediately after the transformation from transmission to photographic density. Area coverage is

achieved by moving the table perpendicular to the Reticon array. The positioning of the table is done open-loop: the commands issued to the motors determine the absolute position of the plate.

### 3.2 Positional repeatability

The overall position repeatability is better than  $1\ \mu\text{m}$  in both directions. The evidence for this is illustrated in Fig. 1 which shows a plot of the density measured in individual ( $10\ \mu\text{m}$ )<sup>2</sup> pixels in two completely independent scans of an identical area on a plate (without taking the plate out of the machine between the scans, and without any change in the mechanical adjustments of the optical system). The choice of the plate used here was dictated by two requirements: first it must have a reasonable range of densities and, secondly, it must be intrinsically noisy to enhance the sensitivity to positional mismatch. The IIA-O plate that we used had a rather large point-spread function in the exposure. The FWHM of the cloud of points is of the order of  $0.01D$ , i.e. more than an order of magnitude below the plate noise. This illustrates the high precision with which both intensities and positions can be reproduced by the Astroscan.

The cloud of points in Fig. 1 is wider than would be expected on the basis of the typical value of the read-out noise of the Reticon array, which is only  $0.001D$ . Therefore, the width in Fig. 1 must be due to the lack of perfect coincidence between the pixels in the respective scans. The emulsion used in this experiment was IIA-O, which has a  $\sigma_D$  of about 0.04 per 1000  $\mu\text{m}^2$  (Le Poole 1980). We therefore

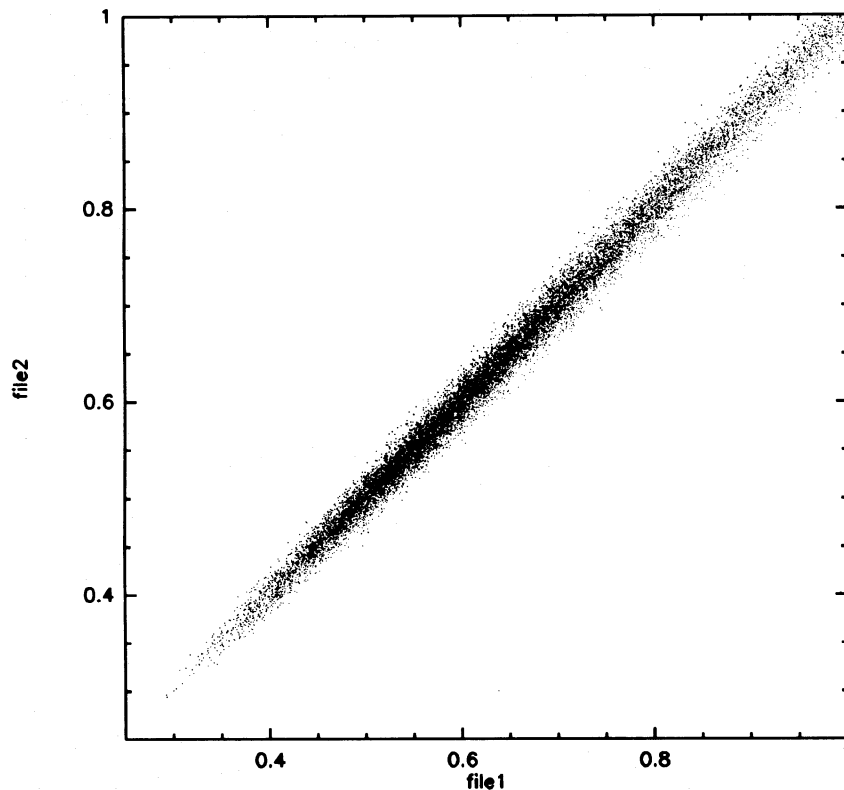


**Figure 1.** The positional repeatability of the Astroscan, as demonstrated by a pixel-by-pixel comparison of the photographic densities measured during two sessions on the same plate (IIA-O emulsion). The scatter in  $\delta D$  is consistent with a read-out noise of the diodes of  $0.001D$  and a positional repeatability of about  $1\ \mu\text{m}$ , which lead to an rms scatter of well below  $0.01D$ .

conclude that the average position repeatability of our  $(10 \mu\text{m})^2$  pixels is better than about  $1.5 \mu\text{m}$ .

### 3.3 Photometric stability and repeatability

In order to exploit the full photometric potential of the machine, accurate set-up and calibration are required. First, the level of the lamp needs to be adjusted for maximum dynamic range. This means that the lamp is set to the highest level at which no saturation of the AD converter of the Reticon array occurs. Secondly, this lamp setting is calibrated by means of a set of neutral density filters with known transmissions. Finally, the zero points of the individual diodes are improved from scanning in the along-array direction. After application of this correction, different diodes measure the same density for a given pixel to better than  $0.001D$ .

Even in the case of the most careful start-up and photometric calibration there are limits to the photometric reproducibility of the Astroscan measures. Clearly, it is impossible to maintain perfect rotational and translational alignment to much better than a few  $\mu\text{m}$ , even for two measurements of the same plate if the plate is taken out of the machine in between the measurements. For example, rotational misalignment of two plates at a level of  $0.001$  can cause shifts of up to  $3\text{--}4 \mu\text{m}$  on a baseline of  $20 \text{ cm}$ . When using film, humidity changes cause scale changes that can be as large as  $20 \mu\text{m}$  over  $20 \text{ cm}$ . Thermal effects on plate scale are negligible as the thermal stability of the Astroscan and its environment is better than  $0.1^\circ\text{C}$  on time-scales of up to 3 months.

### 3.4 Measuring strategy and on-line reduction

The on-line reduction consists of background computation, background subtraction and object detection. For these operations, the area to be scanned is subdivided into a number of basic matrices of  $1024^2$  pixels. These matrices are

reduced while the machine simultaneously scans the next matrix.

Maximum sensitivity for object detection is attained when the effective area of a pixel equals that of the point-spread function (PSF) of the recorded image. If the PSF has been oversampled by a factor of about two (Nyquist sampling), a running mean is taken over  $2 \times 2$  pixels before any further processing takes place. In the case of a typical UKSTU IIIa-J plate, the combination of the telescope seeing and emulsion results in the PSF of about  $(25 \mu\text{m})^2$ , so our basic  $(10 \mu\text{m})^2$  pixels are the obvious choice for recording.

Next, the basic matrix (of  $1024^2$  pixels) is subdivided into submatrices. The size of each submatrix can range from  $16 \times 16$  to  $128 \times 128$  pixels, and is chosen on the basis of the required spatial frequency cut-off in the background map, thereby defining the maximum size of 'objects' to be detected subsequently. For each submatrix we determine an unbiased estimate of the background (sky) density and the local  $\sigma_D$  (see de Vries 1987 for details).

The procedure described above yields a background map with a resolution that is coarser than that of the original by a factor of between 16 and 128. Before we can subtract this background map from the original, a two-step interpolation routine is performed to produce a background map with  $10\text{-}\mu\text{m}$  resolution. In the first step, a proper interpolation of the background map to  $1/4$  of the full resolution is carried out taking into account that the mean positions of the pixels used in the background estimate do not necessarily coincide with the submatrix centres. Secondly, a linear interpolation is performed to the full resolution.

After subtraction of the background, objects are searched for above various threshold levels. A threshold is defined either in terms of the local  $\sigma_D$  or as a nominal level above sky. Objects are defined as one or more adjacent pixels above this threshold. For each of these we store a number of parameters such as the number of pixels above threshold and the zeroth,

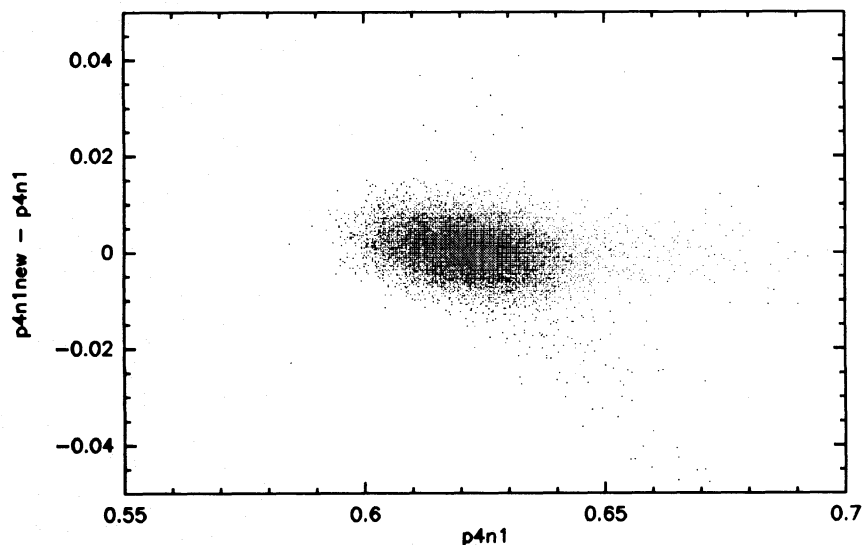


**Figure 2.** The photometric repeatability of the Astroscan, as demonstrated from a comparison of sky backgrounds determined in  $0.32^2 \text{ mm}^2$  pixels, measured on the same plate during two sessions separated by more than four months. As the machine was refocused and photometrically recalibrated between the measurements, the dispersion of  $0.002D$  is a measure of the noise contribution of the real-time background estimation algorithm. Outliers are due to dust, and the slight slope is due to a difference in colour of the illumination in the two experiments, which becomes visible as the exposed plates are not perfectly grey.

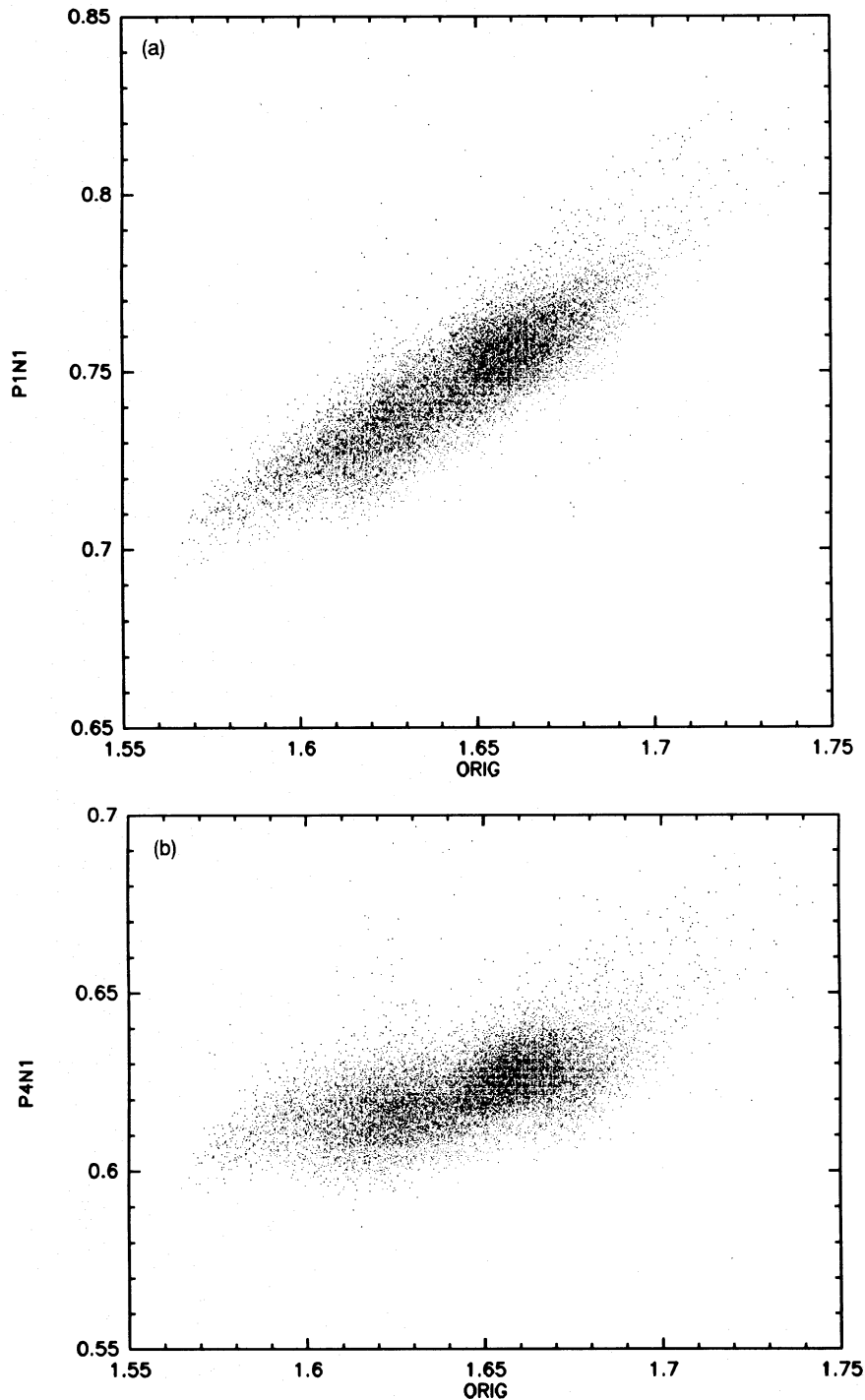
first and second moments. The object positions are derived from the first moment of pixels above the threshold.

#### 4 A COMPARISON OF A UK SCHMIDT PLATE AND ITS COPIES

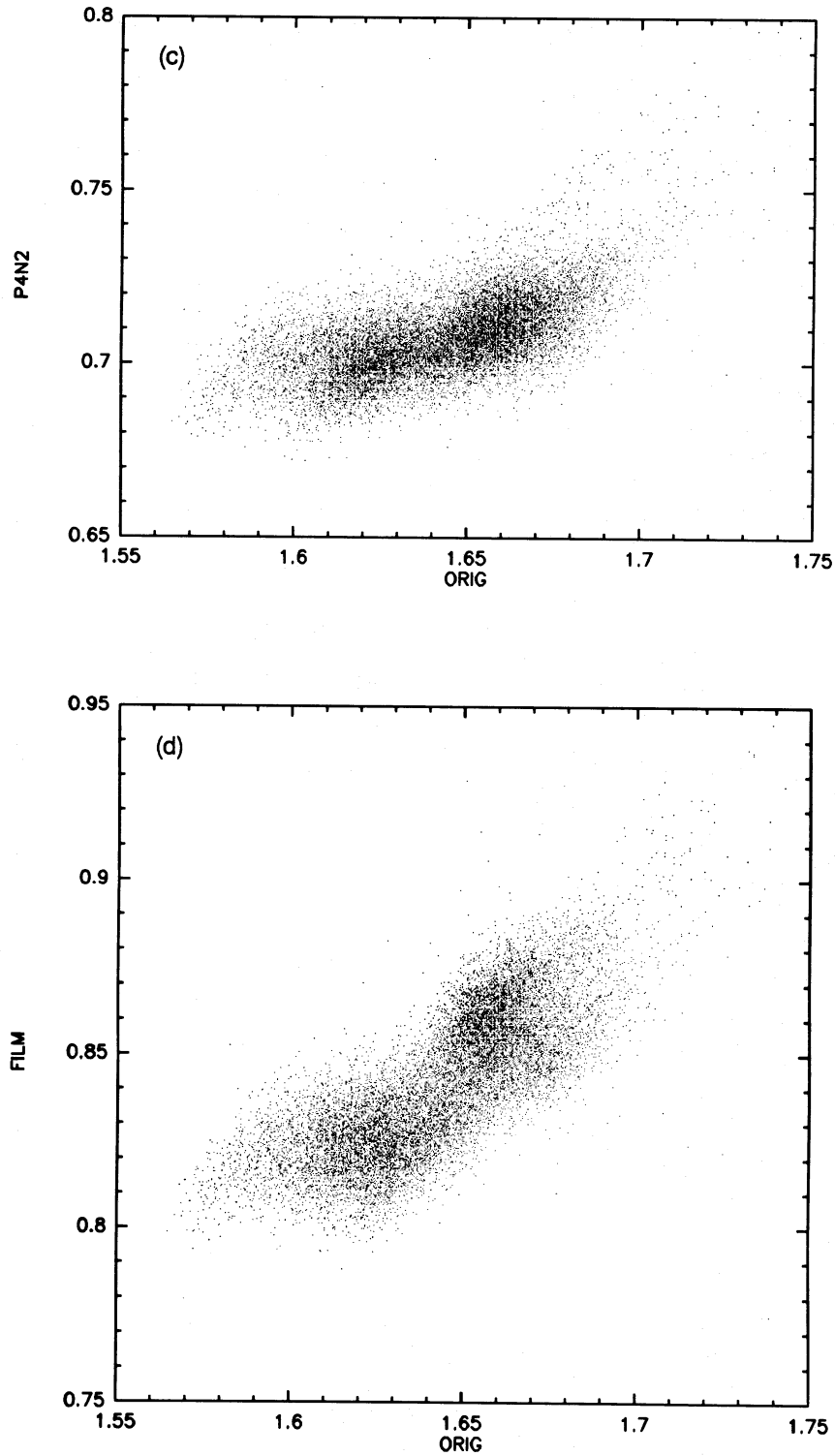
We have used the Astroscan and the on-line reduction software described in the previous section to carry out a detailed

study of the astrometric and photometric fidelity of glass and film copies of an original UKST IIIa-J plate. We used the following photographic material:

- (i) an original IIIa-J plate no. J1681 (denoted by O);
- (ii) two glass negatives made through intermediate positive number 4 (P4N1 and P4N2);
- (iii) a film negative made through intermediate positive number 4 (P4F); and



**Figure 3.** The photometric fidelity of copies, as illustrated by  $D_{\text{copy}}$  versus  $D_{\text{original}}$  for values of the sky background estimated in corresponding  $(0.32 \text{ mm})^2$  areas on the original and the copies. Note that a copy with a 'gain' of 1 should give a slope of unity.

Figure 3 - *continued*

(iv) a glass negative made through intermediate positive number 1 (P1N1).

All copies made of positive P4 were produced at the Atlas laboratory of ESO as 'Atlas quality copies' (see e.g. West 1978). Copy P1N1 and positive P1 were made in Siding Spring in 1975, and positive P4 was also made in Siding Spring in 1978 for Atlas production at ESO. We scanned the

same  $20 \times 20$  cm<sup>2</sup> area on each of these. Overall errors in coincidence, mostly due to scale differences and partly due to rotational misalignment, were less than  $20 \mu\text{m}$  over the entire area.

Before entering into the detailed discussion of the comparison, we want to stress again that we make the fundamental comparison, i.e. the quality of the transfer of the

properties of the grainy silver deposit on an original (in other words: the characteristics of the distribution of the silver) to copies. Any plate, irrespective of the details of the exposure and developing process thus qualifies as an original. Archive portraits of e.g. great astronomers of the turn of the century would do very nicely. Any comparison in terms of derived parameters, such as object positions and magnitudes (or the size of the freckles of e.g. de Sitter), involves an interpretation of the detailed effects of the algorithms defining such quantities (as in e.g. Lee & Van Altena 1983), and is thus necessarily incomplete.

#### 4.1 Photometric comparison

With the plate centre of J1681 near the south Galactic pole, the object density is rather low. We have chosen the 40 per cent lowest pixel values from the histogram on which to base

the estimates of the sky background, and a size of the background submatrices of  $32 \times 32$  pixels. This implies that each background value is based on  $40\,000 \mu\text{m}^2$ , which have been selectively chosen from an area of  $100\,000 \mu\text{m}^2$ . We therefore expect that for a IIIa-J emulsion (with  $\sigma_D/1000 \mu\text{m}^2$  of about 0.03) the noise-induced uncertainty in the background values is about  $0.005D$ .

The first test we applied was a check on the reproducibility of the Astroscan and its on-line software. In Section 3.2 (see also Fig. 1) we have already shown that the Astroscan is capable of reproducing individual pixel values of photographic density with an error which is typically an order of magnitude less than the noise of the emulsion.

For our present purpose we cannot perform the same pixel-by-pixel comparison. However the values of the background calculated for a large area are hardly influenced by the quality of the pixel coincidence (as mentioned above,

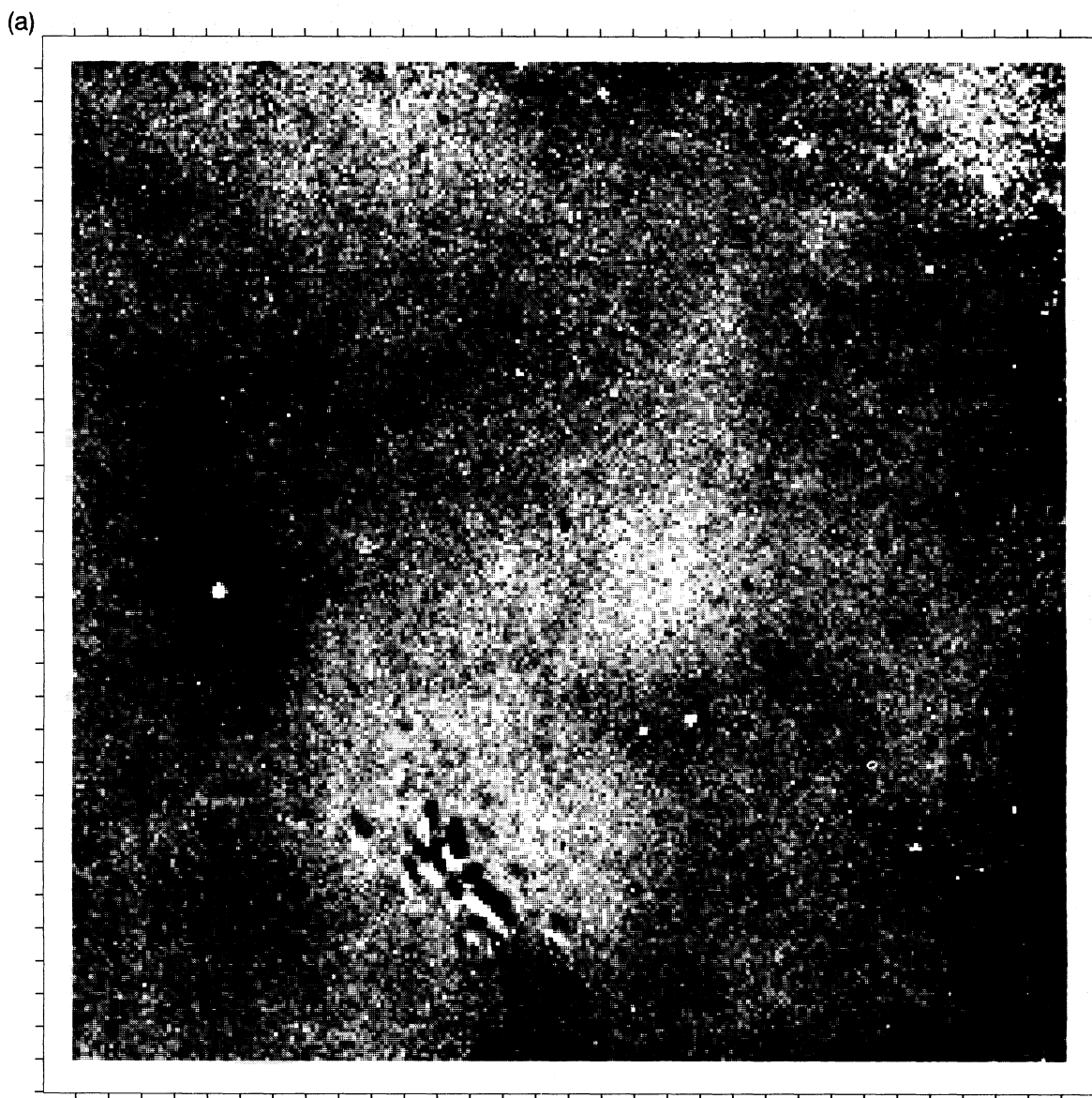


**Figure 4.** The spatial structure in the photometric copying errors. The plots show  $\delta D = D_{\text{orig}} - D_{\text{copy}}$  as a function of position, after transformation of  $D_{\text{copy}}$  to a supposed 'gain' of unity, for which we used the global relation between the densities on both emulsions as shown in Fig. 3, read from smooth fits by hand to the clouds of points.

position differences of up to  $20\ \mu\text{m}$  are possible between plates and film on scales of 20 cm). Therefore, the values of the sky background are clearly the most reliable ones for photometric comparisons to levels well below the noise of the emulsions.

In Fig. 2 we show the result of a comparison of two independent measurements of the same area on P4N1. In between the measurements, the plate was taken out of the machine, and the machine was again set up and calibrated. We plotted the difference between the background estimates found in a  $(7.7\ \text{cm})^2$  subarea of the total area scanned as a function of one of the two background densities. The two measurements were made more than four months apart and are therefore entirely independent as far as the measuring machine is concerned. The standard deviation of the distribution is about  $0.002D$ , with some outliers due to dust. With an estimated value of the  $\gamma$  of the copy of 0.6 (see Fig. 3b) we expect a noise-induced uncertainty of the background estimates of  $0.003D$  for this copy plate. Since the same back-

grounds were measured twice, with a positional mismatch of at most 10 to  $20\ \mu\text{m}$  (compared with a background size of  $320\ \mu\text{m}$ ), we would expect in Fig. 2 a standard deviation of not more than 5 to 10 per cent of the noise-induced uncertainty in the individual backgrounds of  $0.003D$ , i.e. of between  $0.0001D$  and  $0.0003D$ . Clearly, the actual width in Fig. 2 is about a factor of 10 larger than would be expected, and the cause may well be that the background estimation algorithm is more sensitive to the actual selection of the 40 per cent of the pixels than we hoped. Note that the width in Fig. 2 is almost as large as the expected noise of the copy plate, i.e. as if the pixels of the sky background were largely uncorrelated.

The slight slope in Fig. 2 is due to a slight change in colour of the lamp with lamp current, which is visible because photographic emulsions are not perfectly grey absorbers. This colour change causes a change in the definition of the unit of photographic density. However, density scales at different lamp colours map linearly on to each other.

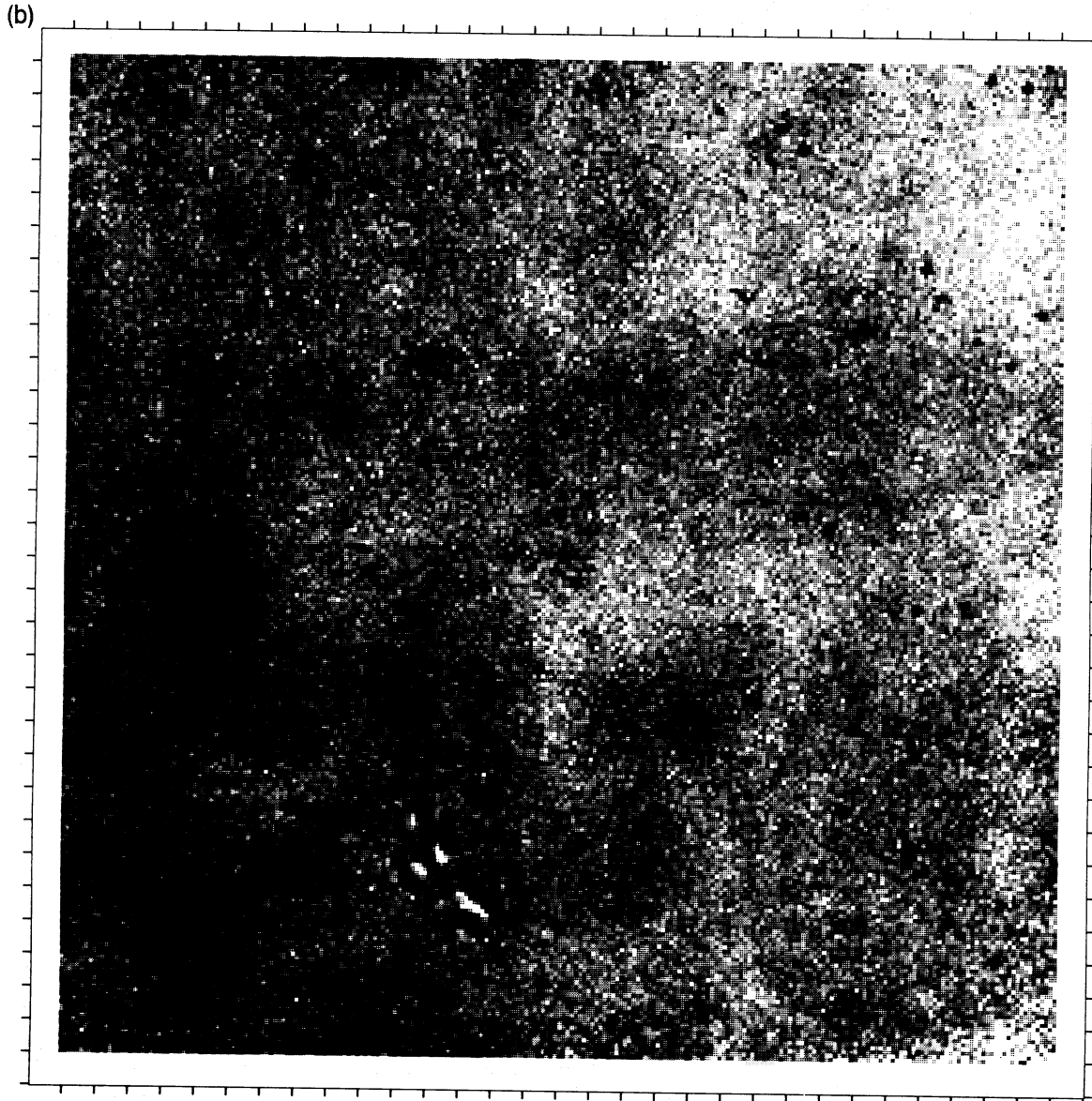


Figure 4 – *continued*



Next a similar comparison was made for the original plate and the copies thereof. The results are shown in Fig 3(a) to (d). In each case the vertical axis shows  $D_{\text{copy}}$  and the horizontal axis  $D_{\text{original}}$ . It is clearly visible that the density range on all copies has been compressed, i.e. the 'gain' (defined as the density range on the copy divided by the corresponding density range on the original) is less than unity, and sometimes as low as about 0.3. Copy P1N1 is clearly the best copy of the original. Not only does it have a fairly well-defined gain but it is also the copy in which the 1-1 mapping of the original density distribution has been achieved most successfully. Both negatives made from intermediate positive number 4 have a hint of bimodal distributions in the scatter diagrams, which imply local inhomogeneities, most likely in the positive, that cause shifts in the respective zero-points of the density scales. These can be due either to position-dependent copying errors or to intrinsic effects in the copy emulsions. However, in all glass copies typical copying errors

are of the order of  $0.01-0.02D$  at most. On the other hand, the film copy P4F (see Fig. 3d) quite clearly shows larger copying errors. The distribution of points in Fig. 3(d) is clearly bimodal with a separation between the two loci of  $0.03-0.04D$ . Since this copy was made through the same intermediate positive as two of the glass copies (which show the same effect to a much lesser extent) it is clear that the errors were caused in the final copying step, in which the film negative was produced from the intermediate positive.

The scatter diagrams in Figs 3(a) to (d), although instructive in themselves, do not shed much light on the spatial distribution of the copying errors. The grey-scale plots in Fig. 4 are designed to give information on this latter aspect. They were produced by subtracting one background map from another after scaling one on to the other on the basis of the data in Figs 3(a) to (d) which represent average transformations. The scaling was performed using a manual fit to the points in Fig. 3. The approximately linear feature in the

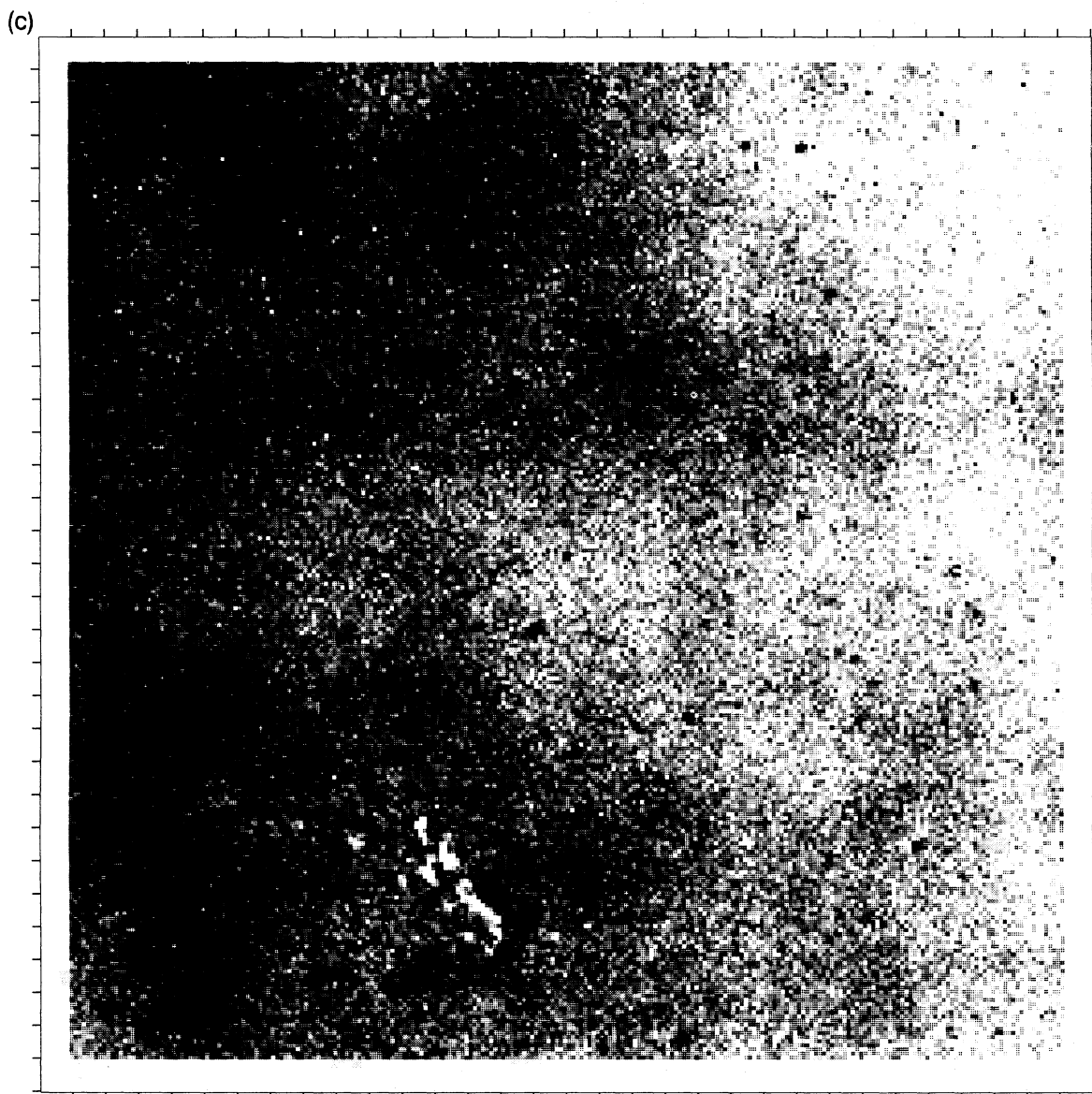


Figure 4 - continued

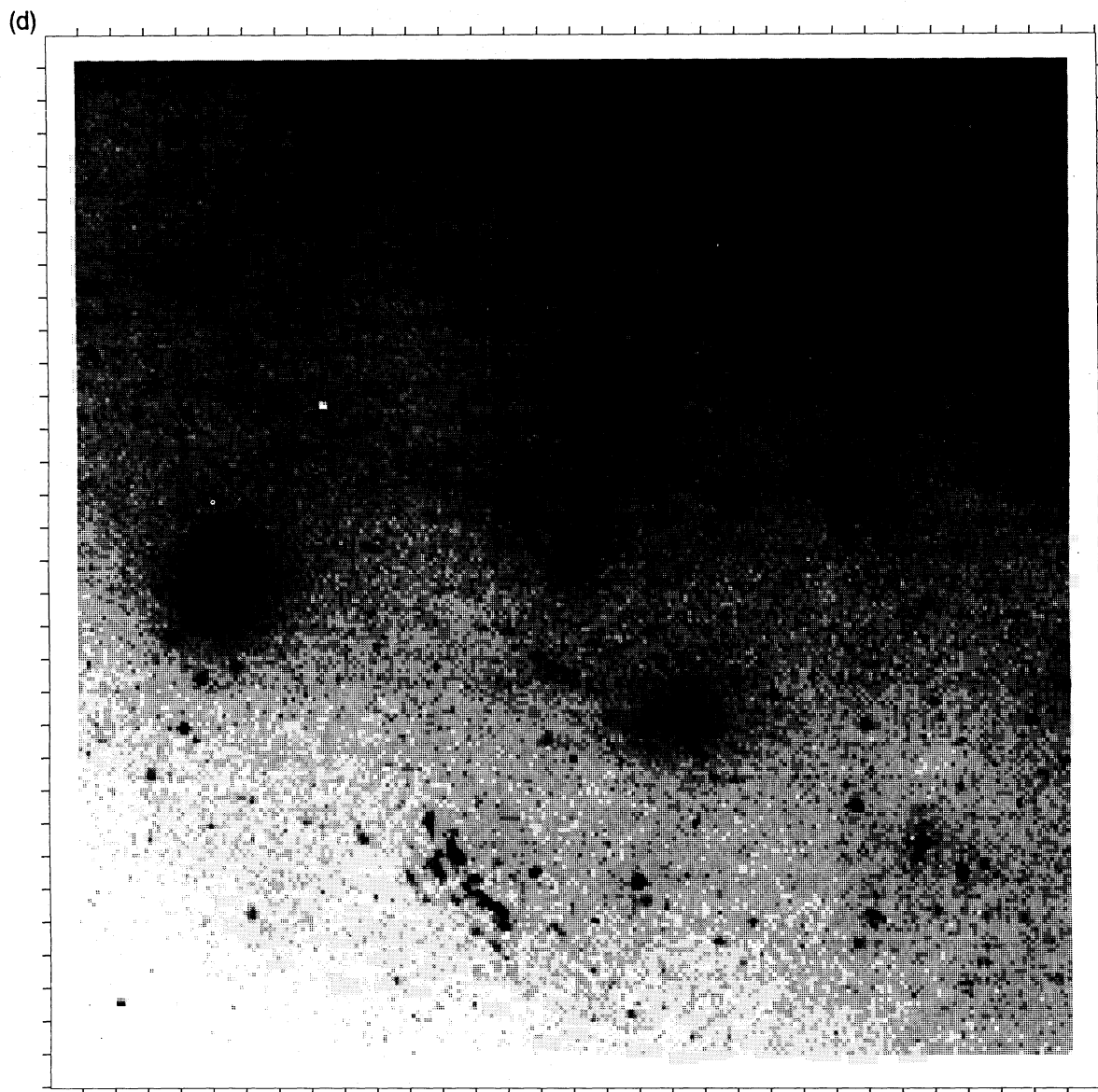


Figure 4 - continued

lower part of the plots (around 150, 50) is caused by an out-of-focus scratch in the support plate used for the glass plates. It is clear that the photometric infidelities have a low-frequency character, with characteristic scales of several centimetres. Note that bright stars are still visible in cases where their size exceeds  $320\ \mu\text{m}$ , the size of a sky submatrix, since they then define the background themselves.

#### 4.2 Astrometric comparison

On the basis of the distribution of objects detected over the entire  $20 \times 20\ \text{cm}^2$  area, we carried out a second investigation, this time into the astrometric fidelity of the copying process. The object search routine used a threshold at six times the local  $\sigma_D$ . On average 250 objects were found per  $\text{cm}^2$ . After weeding out the small objects (less than 20 pixels) and

the very large ones (more than 3000 pixels), which both have larger positional uncertainties than the average object, a cross-identification was performed for each  $\text{cm}^2$  separately. After rejection of doubtful cross-identifications, between 50 and 100 objects per  $\text{cm}^2$  remained. The average displacement in both directions was calculated yielding a pattern of displacement vectors with a sampling of one per cm. With an uncertainty of  $1\text{--}2\ \mu\text{m}$  per object, we estimate that the accuracy of the average position difference in each  $\text{cm}^2$  is around  $0.2\ \mu\text{m}$ .

The resulting vector fields were initially dominated by effects due to non-zero residual rotation, scale differences and translation. To correct for these effects we applied a least-squares fit of what we call a 'limited' transformation between both coordinate systems which allows for a translation, a rotation and an isotropic scale factor. Except when

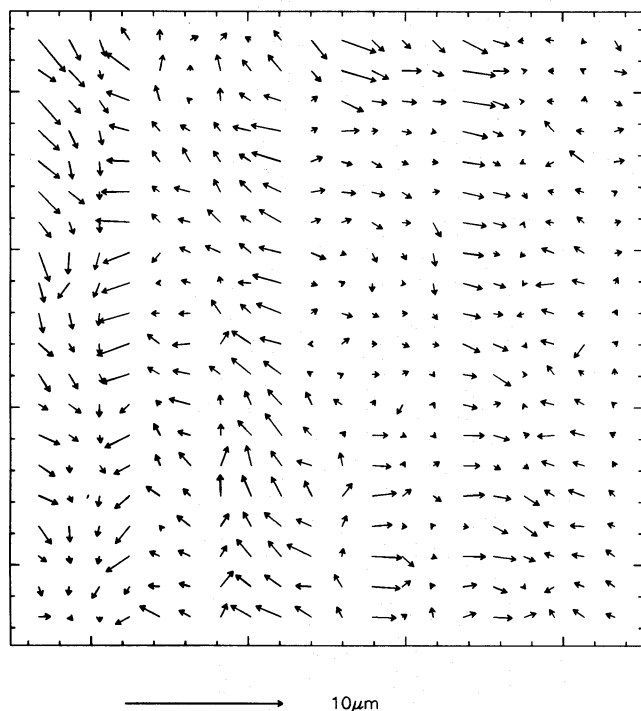


**Figure 5.** The astrometric stability of the Astroscan and the photographic emulsion, expressed as average position difference vectors per  $\text{cm}^2$ , resulting from a comparison between two measurements of the same plate separated by more than four months. The vertical pattern (with an rms amplitude of about  $0.3 \mu\text{m}$ ) is caused by unevenness in the ball-bearings that support the table.

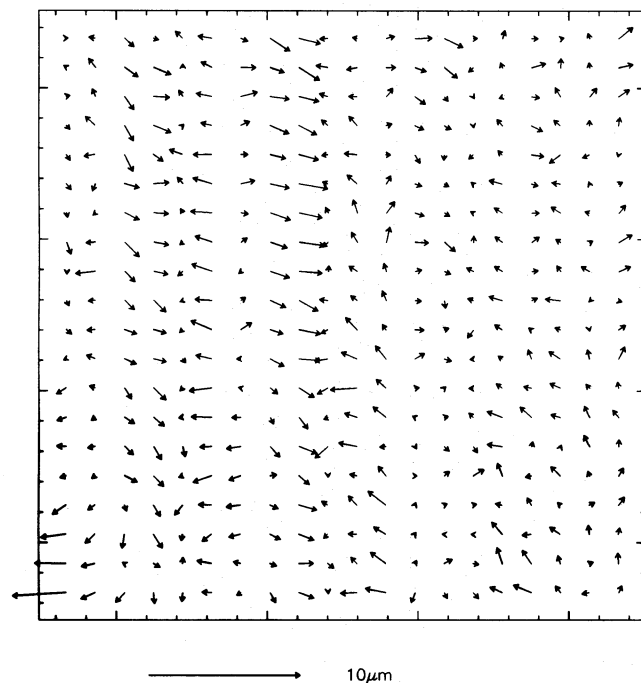


**Figure 6.** The astrometric fidelity of the copying of a positive on to a negative, quantified by the average position difference vectors for each  $\text{cm}^2$ , between copies P4N1 and P4N2. Note that a rotation, isotropic scale and translation have already been accounted for in these vector plots.

indicated otherwise, the vector fields in Figs 5 to 8 represent residuals remaining after application of such a limited transformation.

A 'general' transformation with a non-isotropic scale and a position angle for the anisotropy should not be made since there is no *a priori* reason why such anisotropy should come about in the copying process. If one has to resort to such a general transformation in order to reduce the vector field below the measuring error this indicates a copying error rather than a characteristic of the copying process.

Fig. 5 shows the stability of the Astroscan and the photographic emulsion over a period of more than four months, but now in an astrometric sense. The two object databases compared were generated from the same plate (the glass original). After application of the 'limited' transformation maximum errors of  $1\text{--}2 \mu\text{m}$ , with an rms of  $0.3 \mu\text{m}$  (note the scale) remained. These are instrumental errors which are known to be due to unevenness of the ball-bearings which support the table.

A comparison of P4N1 and P4N2, two glass negatives made through the same intermediate positive, shows a vector field of similar magnitude (see Fig. 6). This leads us to conclude that in principle the copying of a positive onto a negative is possible without errors larger than a small fraction of a  $\mu\text{m}$ .

This immediately leads to the following question: what about a glass and film copy made through the same positive? In the case of film one may expect a loss of positional quality for several reasons. First the material is stressed non-isotropically in the processing machine and this effect may show some hysteresis. Secondly the emulsion is supported by a material that is mechanically weaker and which may not fully resist the stresses (potentially non-isotropic and locally variable) that are induced by temperature and humidity effects on the emulsion. In our experiment, these effects have been minimized because the local environment was kept quite stable in this respect, as the film was placed between two glass plates.

The pattern shown in Fig. 7(a), which shows the vector field for the P4N1–P4F comparison, is not entirely unexpected. It reflects an expansion in one and a constriction in the orthogonal direction. This effect can be accounted for by a non-isotropic scale. After the application of a general transformation the residual vectors [shown in Fig. 7(b), note the different scale] are almost comparable to those in the P4N1–P4N2 comparison (see Fig. 6), and only slightly worse than the reproducibility of the Astroscan itself.

A third and final comparison, between the original and the glass copies, addresses the accuracy with which intermediate positives resemble the original. The two relevant comparisons are shown in Figs 8(a) and (b). These figures show error patterns with infidelities in excess of  $5 \mu\text{m}$  ( $0.34 \text{ arcsec}$ ). As the intermediate positive in this case is a glass positive, these displacements must arise somewhere in the copying process, and can hardly be attributed to anisotropies in the material. In one case (P1N1), as with the film copy, the position errors can be considerably reduced by applying a general, anisotropic, transformation. As stated earlier, this is most likely a signature of a copying error, possibly caused by flexure during the exposure of the intermediate positive of the assembly that holds the plates. However, this does not explain why the residuals, after the general transformation, are larger than in

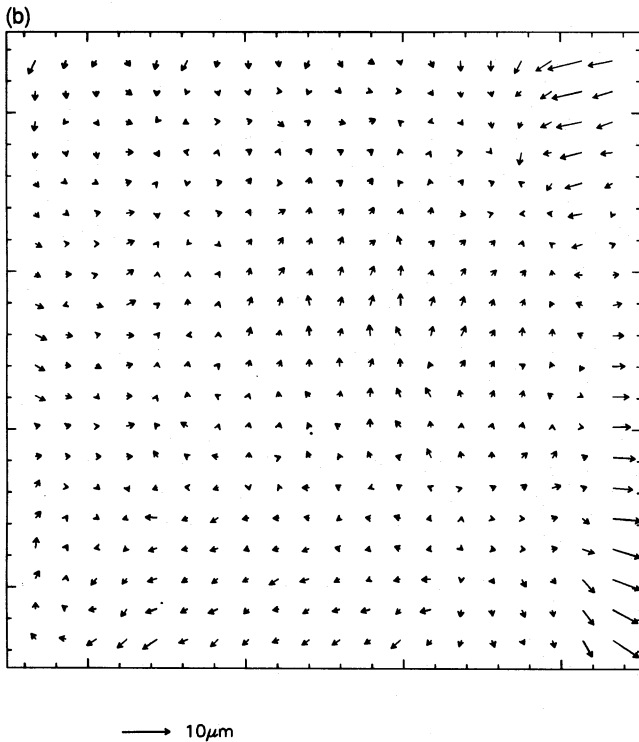
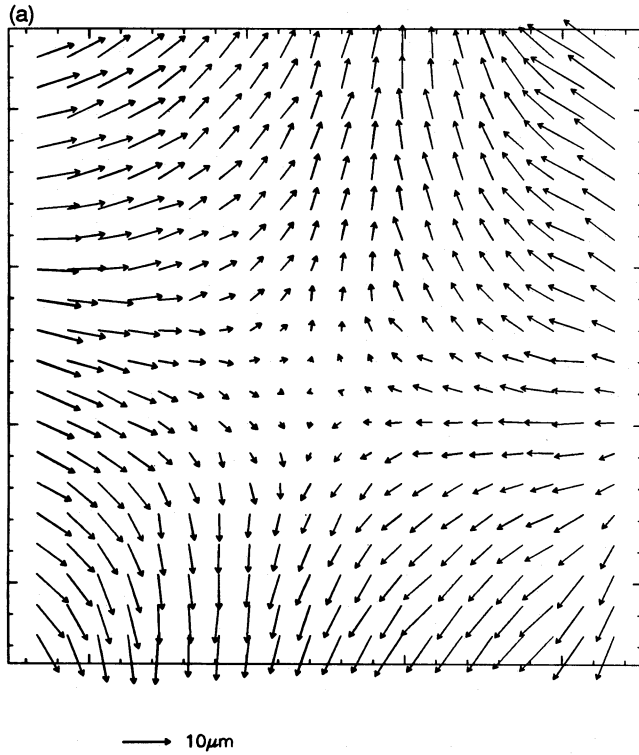


**Figure 7.** A comparison of the astrometric fidelity of the copying of a positive onto glass and film, i.e. of P4N1 and P4F, displayed in the same form as the data in Fig. 6. Note that in the first case (Fig. 7a) an isotropic scale was solved for (in addition to rotation and translation), while in the second transformation an anisotropic scale was allowed for (Fig. 7b).

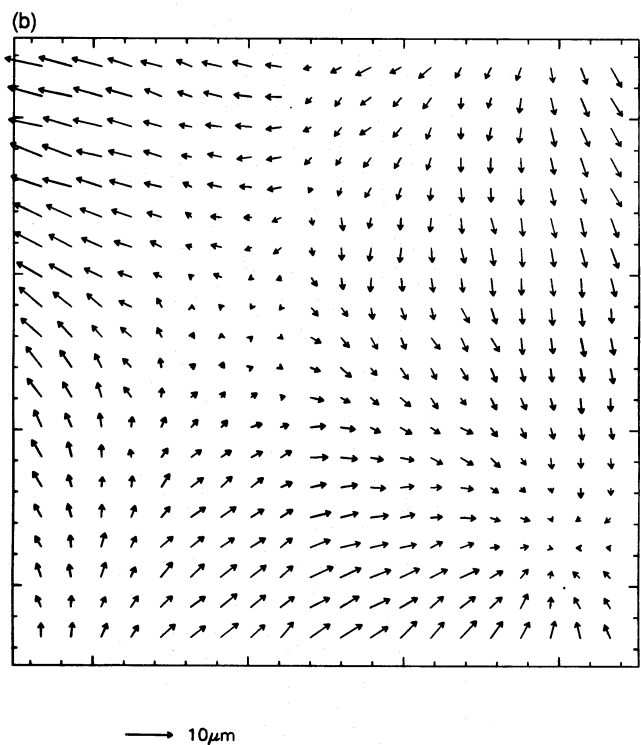
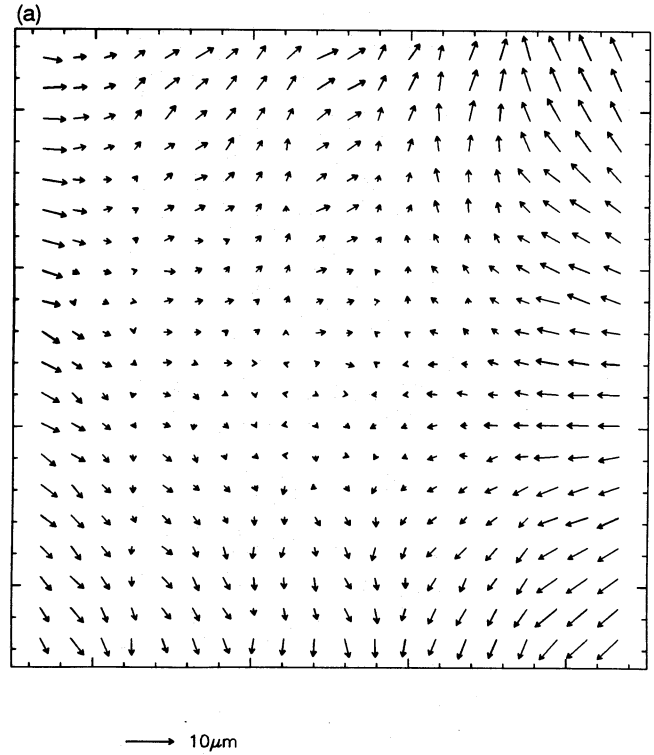


**Figure 8.** The astrometric fidelity of the copying of the original on to the intermediate positives from which the negative glass copies derive, i.e. comparing the original with P1N1 and with P4N1. In both cases only an isotropic scale was allowed for in addition to rotation and translation.

the case of the film copy. In addition, the errors in P4N1 (the copy made via the other intermediate positive) cannot be significantly reduced by a general transformation, and therefore remain completely unexplained.

## 5 CONCLUSIONS

From a careful photometric and astrometric comparison of a UK Schmidt IIIa-J plate and its glass and film copies we conclude that, even in high-fidelity copies produced by the ESO photographic laboratories and the UK Schmidt Unit some photometric and astrometric infidelity is unavoidable. Photometrically, most of the copies have a rather low gain near sky, but the copies are otherwise 'true' at a level of about  $0.02D$ . A film copy shows larger photometric infidelities of up to  $0.03$ – $0.04D$ , and the spatial structure in a plot of the differences has scales of 5 to 10 cm. Astrometrically, all copies are 'true' to a level of  $10\ \mu\text{m}$ . Large-scale anisotropy is visible in the film copy and one glass copy, but this can be reduced to a level of a few  $\mu\text{m}$  by allowing for anisotropic stretching. Even the glass copies show deformations at a level of several  $\mu\text{m}$ ,

most likely originating in the production of the intermediate positives.

## ACKNOWLEDGMENT

MPvH was supported by the Netherlands Foundation for Astronomical Research (ASTRON) with financial aid from the Netherlands Organization for Scientific Research (NWO).

## REFERENCES

- Latham, D. W., 1978. In: *Modern Techniques in Astronomical Photography, Proc. ESO Symp.*, p. 141, eds West & Heudier.
- Lee, J.-F. & Van Altena, W. F., 1983. *Astr. J.*, **88**, 1683.
- Le Poole, R. S., 1980. In: *Two-Dimensional Photometry, Proc. ESO Workshop*, p. 3, eds Crane & Kjär.
- Millikan, A. G., 1978. In: *Modern Techniques in Astronomical Photography, Proc. ESO Symp.*, p. 287, eds West & Heudier.
- de Vries, C. P., 1987. *PhD thesis*, Leiden Observatory.
- West, R. M., 1978. In: *Modern Techniques in Astronomical Photography, proc. ESO Symp.*, eds West & Heudier.